Journal of Hydrology 209 (1998) 186–199

Multicomponent reactive transport in discrete fractures: I. Controls on reaction front geometry

Carl I. Steefel[a,*], Peter C. Lichtner[b,1]

[a]Department of Geosciences, University of South Florida, Tampa, FL 33620, USA
[b]Center for Nuclear Waste Regulatory Analyses, Southwest Research Institute, San Antonio, TX 78238-5166, USA

Received 19 June 1997; received in revised form 24 March 1998; accepted 1 April 1998

Abstract

A multicomponent reactive transport model with mixed equilibrium and kinetic reactions is used to analyze alteration front geometry in discrete fracture-matrix systems. An analytical solution is used to verify the numerical model and to obtain an expression for mineral reaction front geometry under quasi-stationary state conditions. Both the analytical solution and numerical results suggest that the geometry of reaction fronts in a discrete fracture system can be characterized by the sum of two dimensionless parameters: $\phi D'/\delta v$ (ϕ = porosity, D' = effective diffusion coefficient in rock matrix, δ = fracture aperture half-width, and v = fluid velocity in the fracture) and λ_m/λ_f^0 (λ_m = equilibration length scale in rock matrix and λ_f^0 = equilibration length scale in the fracture in the absence of matrix diffusion). In the case where the system is surface reaction-controlled, the first dimensionless parameter, which is independent of the reaction rate constants, dominates. From an analysis of a system described by linear reaction rates, this parameter can be used to predict quasi-stationary state concentration profiles and the distribution of minerals along the length of a fracture based on the one-dimensional diffusion-reaction profile in the rock matrix bordering the fracture. Numerical simulations of a multi-component problem involving dedolomitization resulting from the infiltration of hyperalkaline groundwater demonstrate that the dimensionless parameter $\phi D'/\delta v$ applies in more complicated multicomponent systems as well. This result suggests that field observations of matrix alteration perpendicular to the fracture may be used to predict mineralization along the fracture itself.

Keywords: Fractures; Wall-rock alteration; Solution transport; Mass transfer; Hydrochemistry

1. Introduction

Fractures are extremely important in the transport of contaminants in groundwater systems. This is particularly true where fractures are developed in otherwise relatively impermeable rock of the kind frequently chosen as host rocks for nuclear waste repositories. In such cases, the permeability represented by the fractures is orders of magnitude larger than the permeability of the rock matrix, whereas the bulk rock fracture porosity is much smaller than the matrix porosity. A growing body of work is devoted to understanding the physics of transport in fracture systems (Neretnieks, 1980; Tang et al., 1981; Neretnieks et al., 1982; Moreno et al., 1985; Moreno et al., 1988; Moreno et al., 1990; Skagius and Neretnieks, 1986; Tsang and Tsang, 1989; Cacas et al., 1991; Cvetkovic, 1991; Dykhuizen, 1992; Thoma et al., 1992; Moreno

* Corresponding author.
[1] Present address: Los Alamos National Laboratory, P.O. Box 1663, Mail Stop C305, EES-5, Los Alamos, NM 87545, USA.

PII S0022-1694(98)00146-2

and Neretnieks, 1993; Maloszewski and Zuber, 1993; Therrien and Sudicky, 1996; Nordqvist et al., 1996; Vandergraaf et al., 1997; Park et al., 1997; Odling and Roden, 1997), but a much smaller amount of research has been devoted to examining the coupling of multicomponent chemical reactions and transport in such systems (Novak and Sevougian, 1992; Steefel and Lichtner, 1994; Novak, 1996). Much of the motivation for this work has come from the need to understand the controls on radionuclide transport in the vicinity of nuclear waste repositories.

While flow velocities in fractures are often relatively high, diffusion into the rock matrix can significantly reduce the effective solute velocities in the fracture and retard the rate of contaminant migration (Neretnieks, 1980). Even in the absence of any kind of chemical reaction, the diffusive loss of solutes into the rock matrix bordering fractures may be significant, justifying the need to consider discrete fracture models for transport in fractured media. Matrix diffusion may be even more important in the case where chemical reactions affect the mobility of contaminants, since the rock matrix provides additional sorption and buffering capacity (Neretnieks, 1980; Tang et al., 1981; Steefel and Lichtner, 1994; Novak, 1996).

An issue that arises in assessing the likely performance of nuclear waste repositories is whether the physical and chemical properties of the fractured host rocks will remain constant for the life of the repository (McKinley and Alexander, 1993; Steefel and Lichtner, 1994; Smellie et al., 1997). Because nuclear waste repositories need to function over long periods of times (hundreds to tens of thousands of years), reaction-induced modifications to the physical and chemical properties of the nearfield host rock can become important. In certain cases, significant modifications to the hydrologic and chemical character of the near-field rocks may occur on the time scale of hundreds of years or less. Using one-dimensional reaction-diffusion calculations, Steefel and Lichtner (1994), for example, suggested that the porosity of a rock matrix with a marl composition such as would be found in the near field surrounding the proposed Swiss low-level waste repository could be substantially modified within as little as tens of years. The greatest uncertainty in this estimate appears to be the magnitude of the reacting surface area of minerals used in the calculations. Steefel and Lichtner (1994) pointed to several potential effects, including a porosity increase or decrease in the rock matrix and in the fracture. A porosity decrease in the rock matrix could affect effective solute velocities in the fracture by: (1) decreasing the effective diffusion coefficients for solutes in the matrix, thus reducing the ‘diffusive loss’ to the matrix, and (2) by reducing the amount of reactive surface area on minerals available for both sorption and for dissolution (and possibly precipitation) reactions.

Several different methods have been used to simulate reactive transport in fracture systems. One possibility is to treat the fracture network as an equivalent porous medium (Steefel and Lasaga, 1994). However, the large disparity between fracture and matrix properties would suggest that this approach is of limited utility. Another possibility is to treat transport of reactive fluids in fractured media by focusing on single fractures or sets of fractures. Little has been done, however, to investigate multicomponent reactive transport in these systems. One exception is the work of Novak (1996) and Novak and Sevougian (1992) who considered a relatively complicated multicomponent problem involving adsorption and precipitation/dissolution reactions taking place in both the fracture and the rock matrix. These authors carried out a local equilibrium analysis which showed that precipitation/dissolution reactions in rock matrix coupled via matrix diffusion to solute transport in the adjacent fracture could significantly affect the retardation of solutes in the fracture.

In this paper the one-dimensional reaction-diffusion analysis of Steefel and Lichtner (1994) is extended to include advection, dispersion, and reaction in a single fracture coupled to matrix diffusion and reaction. In their one-dimensional analysis, Steefel and Lichtner (1994) treated the fracture wall as a constant concentration boundary condition, such as would be expected close to the fracture inlet or in the case where fluid velocities in the fracture are sufficiently high. In this study, we relax this assumption and consider the evolution of solute concentrations both along the fracture and in the rock matrix (i.e., a two-dimensional domain). In addition, we present an analytical solution for the explicit fracture system which differs from that presented by Tang et al. (1981) in allowing for

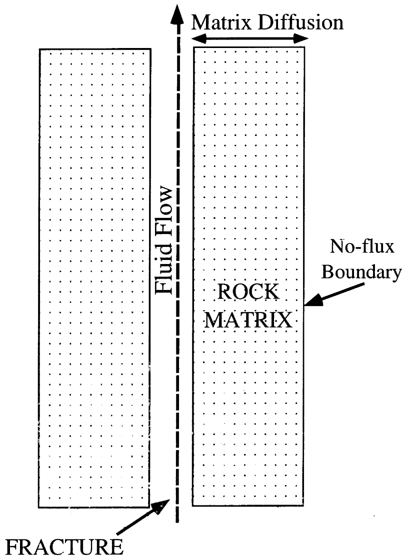

Fig. 1. Schematic representation of a single discrete fracture bordered by low permeability rock matrix.

different reaction rates in the fracture and matrix. The analytical solution is also cast into a series of terms which we believe give greater insight into the physical and chemical controls on alteration front geometry in two-dimensional discrete fracture systems. In a companion paper (Steefel and Lichtner, 1998), we apply these results to an analysis of water–rock reactions in fractured marl at Maqarin, Jordan, a site which has been proposed as a natural analogue to conditions expected in the vicinity of cement-bearing nuclear waste repositories.

2. Physical system

Consider a thin nondeformable fracture developed within saturated porous rock matrix with a significantly lower permeability compared to the fracture such that flow within the rock matrix is negligible (Fig. 1). Solute transport within the rock matrix, therefore, is via molecular diffusion only. The fractures are assumed to have constant apertures and smooth parallel walls initially. In addition we assume in all cases that the width of the fracture is much smaller than its length and that transverse diffusion and dispersion within the fracture cause complete mixing across the fracture width. These two assumptions are used to justify a one-dimensional treatment of mass transport along the fracture (Tang et al., 1981). Unlike the treatment by Tang et al. (1981), however, diffusion is considered to be two-dimensional in the numerical simulations described below. The rock matrix is assumed to have initially homogeneous physical and chemical properties, although this is not a requirement for the numerical model. A chemical source of constant strength is assumed to exist at the inlet to the fracture.

We present a formulation which allows for feedback between mineral reactions and the transport properties of the rock matrix or fracture. In this paper, however, the simulations are carried out without this feedback in order to focus on the behavior of the system within a time frame less than that in which the physical properties of the matrix and fracture are modified significantly. Given a constant hydraulic head gradient across the length of the fracture, this assumption results in a constant flow velocity in the fracture and constant diffusivities in the rock matrix. Although this assumption is not realistic for longer times (even though it is almost always the standard assumption in studies of water–rock interaction, whether explicitly stated or not), it provides an end-member behavior which is useful because it excludes the nonlinear feedbacks associated with time-dependent porosity and permeability change. In addition, it allows us to examine the quasi-stationary state behavior of the system (Lichtner, 1988; Lichtner, 1991). In a companion paper (Steefel and Lichtner, 1998), simulations involving the reaction-induced porosity and permeability change are included.

3. Governing equations

3.1. Formulation for a single fracture

A model which allows for both transport of fluid in the fracture network, as well as diffusive transport in the rock matrix, results in a discrete fracture model. The transport equations for the discrete fracture model include separate equations for the fracture network and the rock matrix. These equations are coupled and must be solved simultaneously. In certain cases, it may be possible to assume that lateral fluxes (parallel to the fractures) within the rock matrix can be neglected because they are small compared to the fluxes perpendicular to the fracture (Tang et al., 1981). In this case, it is possible to reduce the problem to solving a set of coupled one-dimensional problems: one corresponding to the fracture network and the others to one-dimensional diffusive transport perpendicular to the fracture. Since we include lateral diffusive fluxes in the numerical analyses presented in this work, however, we give the governing equations with the lateral diffusive fluxes included.

The differential equations describing the conservation of solute mass in a single fracture can be written as

$$\frac{\partial C_j^{\mathrm{f}}}{\partial t} = -v\frac{\partial C_j^{\mathrm{f}}}{\partial z} + D\frac{\partial^2 C_j^{\mathrm{f}}}{\partial z^2} - \sum_{s=1}^{N_s} \nu_{js} r_s + \frac{\phi D'}{\delta}\frac{\partial C_j^{\mathrm{m}}}{\partial x}\Big|_{x=\delta}, (j=1, \ldots, N_c), \quad (1)$$

and for the rock matrix as

$$\frac{\partial}{\partial t}[\phi C_j^{\mathrm{m}}] = \frac{\partial}{\partial x}\left[\phi D'\frac{\partial C_j^{\mathrm{m}}}{\partial x}\right] + \frac{\partial}{\partial z}\left[\phi D'\frac{\partial C_j^{\mathrm{m}}}{\partial z}\right] - \sum_{s=1}^{N_s} \nu_{js} r_s \quad (2)$$

where z is the coordinate along the fracture, L; x is the coordinate perpendicular to fracture, L; t is the time, T; v is the groundwater velocity in the fracture, L/T; C_j^{f} is the total dissolved concentration of the jth component in fracture, M/L^3; C_j^{m} is the total dissolved concentration of the jth component in rock matrix, M/L^3; ϕ is the rock matrix porosity, dimensionless; N_{s} is the number of reacting minerals in the system; N_{c} is the number of independent chemical components in the system; ν_{js} is the stoichiometric reaction coefficient; r_s is the reaction rate of mineral s, M/L^{3}T; τ is the tortuosity, dimensionless; D' is the effective diffusion coefficient in the rock matrix ($D' = \tau D_{\mathrm{w}}$), M^2/T; D_{w} is the diffusion coefficient in water, M^2/T; and 2δ is the fracture aperture, L.

The dispersion coefficient D is defined according to Bear (1979) as

$$D = \alpha_{\mathrm{L}} v + D_{\mathrm{w}}, \quad (3)$$

where α refers to the dispersivity along the fracture. The porosity in the fracture is assumed equal to unity. In Eq. (1), the last term on the right hand side represents the diffusive flux of component j across the wall of the fracture. Although diffusion in porous media is often described in terms of a 'diffusion porosity' (Norton and Knapp, 1977) or formation factor, F, (Dullien, 1979; Steefel and Lichtner, 1994), in this work we define the diffusion in porous media according to (Bear, 1979)

$$D' = \tau D_{\mathrm{w}}. \quad (4)$$

where τ is the tortuosity of the rock matrix. Note that since the porosity multiplies the diffusion coefficient, D', in Eq. (2), the diffusive flux will $\rightarrow 0$ as the porosity $\rightarrow 0$.

In this formulation, the total dissolved concentrations, C_j, in both the fracture and matrix are defined by assuming equilibrium among the individual aqueous species in the system (Reed, 1982; Lichtner, 1985; Kirkner and Reeves, 1988; Yeh and Tripathi, 1991)

$$C_j = c_j + \sum_{i=1}^{N_{\mathrm{sec}}} \nu_{ij} c_i, \quad (5)$$

where c_j refers to the concentration of the jth primary or basis species, and c_i refers to the concentration of the ith secondary species, of N_{sec} in number.

3.2. Fracture permeability and flow

We assume that fracture permeability is described by the 'cubic law' which states that rate of fluid flow across a section of the fracture is proportional to the applied pressure gradient and the cube of fracture aperture (e.g., Snow, 1968; Phillips, 1991). The permeability for a set of parallel fractures with smooth walls is given by (Snow, 1968)

$$\kappa = \frac{\phi_{\mathrm{f}} b^2}{12} = \frac{nb^3}{12}, \quad (6)$$

where n is the number of fractures per unit distance across the rock (L^{-1}), b is the fracture aperture ($b = 2\delta$), and the fracture porosity, ϕ_{f} is related to the fracture density and aperture by the expression

$$\phi_{\mathrm{f}} = nb. \quad (7)$$

We distinguish here between the *local* porosity of the fracture which is assumed to be unity and the bulk rock (continuum) fracture porosity ϕ_{f} which in general is not equal to one. The situation is more complicated in a real system where fracture walls are either nonsmooth or nonparallel (Ge, 1997) or even in an idealized system, as considered here, where local changes in the fracture aperture due to mineral dissolution and precipitation reactions are included. Although clearly an approximation, we assume that the cubic law holds locally. For practical purposes, the cubic law is assumed to hold over the length of a numerical grid cell along the fracture.

The Darcian flux in a unit volume of porous medium is given by

$$u = -\frac{\rho g \kappa}{\mu}\frac{\partial h}{\partial z} \tag{8}$$

where μ is the fluid viscosity, ρ is the fluid density, g is the gravitational constant, and $\partial h/\partial z$ is the gradient in hydraulic head in the fracture plane (de Marsily, 1986). Since the mean flow velocity v is related to the Darcian flux by

$$v = \frac{u}{\phi_\mathrm{f}} = \frac{u}{nb}, \tag{9}$$

the mean flow velocity can be written as

$$v = -\frac{\rho g b^2}{12\mu}\frac{\partial h}{\partial z} \tag{10}$$

The formulation in terms of a single fracture can be extended to an equivalent porous media in the case where the fractures form a parallel set by multiplying both sides of Eq. (1) by the fracture porosity, $\phi_\mathrm{f} = nb$.

3.3. Initial and boundary conditions

The initial composition of the fluid in the fracture and rock matrix and the mineral composition of the rock matrix must be specified at time $t = 0$. In addition, the composition of the fluid at the inlet to the fracture must be specified. Explicitly, these conditions are represented by the equations:

$$C_j^\mathrm{f}(0,\ t) = C_j^\mathrm{f}(0), \tag{11}$$

$$C_j^\mathrm{f}(z,\ 0) = C_j^\mathrm{f}(\infty), \tag{12}$$

$$C_j^\mathrm{m}(x,\ 0;\ z) = C_j^\mathrm{m}(\infty). \tag{13}$$

At the boundary between the rock matrix and the fracture, the solute concentrations are related by the continuity condition:

$$C_j^\mathrm{m}(0,\ t;\ z) = C_j^\mathrm{f}(z,\ t). \tag{14}$$

Also needed is a boundary condition at some distance in the x direction into the rock matrix. Assuming that the rock consists of a set of equally spaced, parallel fractures, symmetry requires that a zero flux condition exist midway between fractures

$$\frac{\partial C_j^\mathrm{m}}{\partial x}\Big|_{x=d/2} = 0, \tag{15}$$

where d is the fracture spacing ($= 1/n$).

3.4. Kinetic formulation

We use a kinetic rate law based on the assumption that attachment and detachment of ions from mineral surfaces is the rate-limiting step (i.e., a surface reaction-controlled rate law). It does not mean, however, that one cannot obtain overall transport control on the mineral dissolution or precipitation rate since this depends on the magnitude of the reaction rate relative to the macroscopic transport rates. The rate laws used for mineral precipitation and dissolution are based loosely on transition state theory (e.g., Lasaga, 1981; Lasaga, 1984; Aagaard and Helgeson, 1982). This formulation gives the dependence of the rate on the saturation state of the solution with respect to a particular mineral as a function of the ion activity product, Q_s, defined by

$$Q_\mathrm{s} = \prod_{j=1}^{N_\mathrm{c}} a_j^{\nu_{js}}, \tag{16}$$

where the a_j are the activities of the primary species used in writing the dissolution reaction for the mineral. In order to incorporate the strong pH dependence of most mineral dissolution and precipitation reactions far from equilibrium, parallel rate laws are used which are summed to give the overall reaction rate law for a particular mineral

$$r_\mathrm{s} = -A_\mathrm{s}\left\{\sum_{l=1}^{N_\mathrm{rs}} k_l \left(\prod_{i=1}^{N_\mathrm{c}+N_x} a_i^{p_{il}^\mathrm{s}}\right)\right\}\left[1 - \left(\frac{Q_\mathrm{s}}{K_\mathrm{s}}\right)\right], \tag{17}$$

where k_l is the far from equilibrium dissolution rate constant for the lth parallel reaction, p_{il}^s gives the dependence of the lth parallel reaction on a particular species far from equilibrium, K_s is the equilibrium constant, N_rs is the number of parallel reactions, and A_s refers to the surface area of individual minerals in the rock matrix or fracture. A nonlinear dependence on the solution saturation state (e.g., Steefel and Van Cappellen, 1990; Steefel and Lasaga, 1994) can be included, but is not done so here. The term $\Pi_{i=1}^{N_c+N_x} a_i^p$ incorporates the effects of various ions in solution on the far from equilibrium dissolution rate. This is most commonly the solution pH or hydroxyl ion activity but may include other electrolytes as well (e.g., Na^+ and Cl^-; Dove, 1995). As an example, consider the overall rate law for kaolinite (Nagy, 1995) which includes H^+- and OH^--dependent dissolution rates

$$r_{\mathrm{kaol}} = -A_{\mathrm{kaol}}\{k_{\mathrm{H^+}} a_{\mathrm{H^+}}^{0.17} + k_{\mathrm{OH^-}} a_{\mathrm{OH^-}}^{0.54}\}\left[1 - \frac{Q_{\mathrm{kaol}}}{K_{\mathrm{kaol}}}\right]. \tag{18}$$

Note also that Eq. (17) is fully compatible with the thermodynamics of the system, since if the rate constant is chosen large enough relative to the transport rates in the system, local equilibrium (or transport-controlled) behavior is obtained.

Depending on how mineral surface area is computed, it may be necessary to include a dependence of the surface area on the matrix and fracture porosity such that $A_s \rightarrow 0$ as the porosity $\phi \rightarrow 0$. Mineral surface area formulations based on grain size like that presented by Lasaga (1984) cannot be used to describe the mineral surface area in contact with fluid as the porosity goes to zero (a porous medium made up of closest packed spheres cannot have a zero porosity). Here we use the expression

$$A_s(t) = A_s^o\left(\frac{\phi(t)}{\phi_o}\right), \tag{19}$$

where A_s^o and ϕ_o refer to the initial surface area and initial porosity, respectively.

3.5. Mineral alteration equations

The mineral alteration equations for both fractures and the rock matrix have the form

$$\frac{\partial \phi_s}{\partial t} = \bar{V}_s r_s \tag{20}$$

where $\bar{V}_s$ refers to the mineral molar volume. The porosity can be calculated directly from Eq. (19) (assuming no other processes result in a change in porosity) since

$$\phi = 1 - \sum_{s=1}^{N_s} \phi_s. \tag{21}$$

The rate of change of the fracture aperture can be related to the rate of change of the mineral volume fractions in the fracture, ϕ_s^f, by applying Eq. (19) to the fracture to yield

$$\frac{\partial \delta}{\partial t} = -\delta \sum_{s=1}^{N_s} \frac{\partial \phi_s^f}{\partial t} = -\delta \sum_{s=1}^{N_s} \bar{V}_s r_s\ , \tag{22}$$

where ϕ_s^f, refers to the mineral volume fractions in the fracture. In finite difference form, this equation becomes

$$\delta(z,\ t+\Delta t) = \delta(z,\ t)\left(1 - \Delta t \sum_s \bar{V}_s r_s\right). \tag{23}$$

This equation is used when updating the fracture aperture as a function of time and space.

4. Numerical solution method

The governing partial differential equations are discretized using integrated finite differences (de Marsily, 1986). In many cases it is possible to take advantage of the special structure of the discrete fracture problem and to cast the system as a series of one-dimensional reaction-diffusion equations perpendicular to the fracture coupled to a one-dimensional advection-dispersion-reaction equation following the fracture. This is the approach taken in formulating the discrete fracture model for the analytical solutions given below and in Tang et al. (1981). However, in this work we include lateral fluxes (parallel to the fracture) within the rock matrix, making the problem fully two-dimensional. To solve the system, we use a slightly modified version of the code GIMRT (Steefel and Yabusaki, 1996) which uses a global implicit or one-step method to couple transport and reaction (Steefel and Lasaga, 1994; Steefel and MacQuarrie, 1996).

The advantages and disadvantages of the global implicit scheme as compared to other possible approaches to coupling multicomponent reaction and transport are discussed by Steefel and MacQuarrie (1996). As pointed out by Yeh and Tripathi (1989), the principal disadvantage of the global implicit or one-step approach is its use of large amounts of computer memory. The discrete fracture calculations, described in detail in Steefel and Lichtner (1998), for example, required 35 to 45 MB of physical memory. In addition, the CPU time required to complete a single time step is generally larger than the time required for a decoupled approach like the 'one-step' or sequential non-iterative approach (SNIA). The principal advantage of the global implicit approach, however, is its ability to take significantly larger time steps than is possible with the other methods. Because transport is fully implicit, there is no Courant number limitation on the timestep for stability requirements as would be the case where transport was handled explicitly. In addition, the full coupling of reaction and transport terms eliminates operator splitting errors occurring in completely decoupled approaches like the SNIA or two-step approach.

Advective transport in the fracture is handled using a standard first-order accurate upwind formulation. This approach can also add considerable numerical dispersion to the transient solution, making this particular implementation unsuitable for problems where tracking of a transient concentration front is essential at high Peclet number (for this purpose the code OS3D [Steefel and Yabusaki, 1996] with its 3rd order accurate TVD scheme can be used). In this study, however, the principal focus is on quasi-stationary state effects like porosity and permeability change rather than the accurate tracking of transient concentration fronts, so numerical dispersion is not a significant issue. Moreover, even the global implicit upwind scheme employed here performs relatively well because concentration fronts in the fracture are not extremely sharp due to the diffusive loss of solutes to the rock matrix. This can be seen by comparing the results to the analytical solution for the discrete fracture system as we do below.

5. Verification of algorithm against an analytical solution

The analytical solutions for transport in a single fracture and adjacent rock matrix presented by Tang et al. (1981) can be used as a partial verification of the numerical approach outlined here. Tang et al. (1981) give a solution which includes radioactive decay and adsorption described by a linear equilibrium isotherm. Tang et al. (1981) also give solutions for the case in which dispersion in the fracture is included and for the case where it is neglected (since the neglect of dispersion in the fracture admits a simpler analytical solution which need not be integrated numerically). Here we modify the Tang et al. (1981) solution so that radioactive decay is replaced with a mathematically similar linear rate law for precipitation and dissolution of a mineral phase (e.g., quartz or amorphous silica) in a single component system. In addition, we allow for the possibility of the effective rate constant (including both the intrinsic rate constant and the mineral surface area contribution) differing between the fracture and the rock matrix. Assuming pure diffusion, linear reaction kinetics, and constant porosity in the rock matrix (and an assumption of unit porosity in the fracture), the transport equations for the matrix and fracture are given by

$$\frac{\partial C_m'}{\partial t} = D' \frac{\partial^2 C_m'}{\partial x^2} - \frac{k_m}{\phi} C_m' \tag{24}$$

and

$$\frac{\partial C_f'}{\partial t} = -v \frac{\partial C_f'}{\partial z} - k_f C_f' + \frac{\phi D'}{\delta} \frac{\partial C_m'}{\partial x}\bigg|_{x=\delta}. \tag{25}$$

In these equations C_m' and C_f' are defined by and

$$C_m' = C_m - C_m^{eq}, \tag{26}$$

and

$$C_f' = C_f - C_f^{eq}. \tag{27}$$

These equations are subject to the boundary conditions

$$C_f'(0,t) = C_0', \tag{28}$$

$$C_m'(\infty,\ z,\ t) = 0, \tag{29}$$

$$C_m'(0,\ z,\ t) = C_f'(z,\ t) \tag{30}$$

and the initial conditions

$$C_m'(x,\ z,\ 0) = 0 \tag{31}$$

$$C_f'(z,\ 0) = 0 \tag{32}$$

where k_f refers to the rate constant in the fracture.

As noted above, the analytical solutions to these equations take a simpler form when pure advective transport is assumed in the fracture. The transient

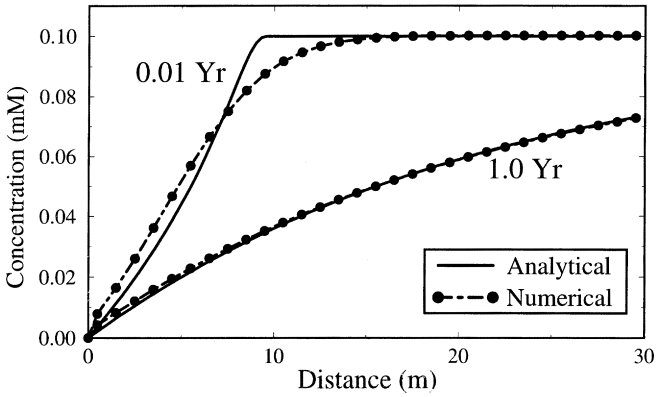

Fig. 2. Comparison of analytical and numerical solutions for quartz dissolution in the fracture at 0.01 and 1.0 years. Discrepancy for early times is due to numerical dispersion in upwind numerical method which disappears as the system approaches steady state at 1 year.

solution for Eq. (24) (the fracture) is given by

$$C_f{}' = 0, (z > vt),$$

$$C_f{}' = \frac{C_0{}'}{2}\left\{\exp\left(-\frac{z}{\lambda_f}\right)\mathrm{erfc}(\xi_+) + \exp\left[-z\left(\frac{1}{\lambda_f^0} - \frac{1}{\mathrm{Pe}\lambda_m}\right)\right]\mathrm{erfc}(\xi_-)\right\},\ (z < vt), \tag{33}$$

with

$$\xi_\pm = \frac{z}{2\mathrm{Pe}\sqrt{D'(t-\frac{z}{v})}} \mp \frac{1}{\lambda_m}\sqrt{D'(t-\frac{z}{v})}, \tag{34}$$

and where λ_f and λ_m are the characteristic equilibration lengths for the fracture and matrix, respectively, defined by

$$\lambda_m = \sqrt{\frac{\phi D'}{k_m}}, \tag{35}$$

and

$$\lambda_f = \frac{1}{\frac{1}{\lambda_f^0} + \frac{1}{\mathrm{Pe}\lambda_m}}. \tag{36}$$

The quantity λ_f^0 refers to the fracture equilibration length in the absence of matrix diffusion given by

$$\lambda_f^0 = \frac{v}{k_f} \geq \lambda_f, \tag{37}$$

and the Peclet-like number, Pe, is defined in terms of the approximate diffusion length scale provided by the fracture aperture half-width

$$\mathrm{Pe} = \frac{v\delta}{\phi D'}. \tag{38}$$

The transient solution to Eq. (23) (the rock matrix) is given by

$$C_m{}' = 0, (z > vt),$$

$$C_m{}' = \frac{C_0{}'}{2}\left\{\exp\left[-\left(\frac{z}{\lambda_f} + \frac{x-\delta}{\lambda_m}\right)\right]\mathrm{erfc}(\eta_+) + \exp\left[-z\left(\frac{1}{\lambda_f^0} - \frac{1}{\mathrm{Pe}\lambda_m}\right)\right]\exp\left(\frac{x-\delta}{\lambda_m}\right)\mathrm{erfc}(\eta_-)\right\}, \times (z < vt), \tag{39}$$

where $\eta_\pm$ is defined by

$$\eta_\pm = \frac{\frac{z}{\mathrm{Pe}} + x - \delta}{2\sqrt{D'(t-\frac{z}{v})}} \mp \frac{1}{\lambda_m}\sqrt{D'(t-\frac{z}{v})} \tag{40}$$

The analytical solution can be compared to the results given by the numerical model described above for the case of reactive transport of a single component (e.g., SiO_2(aq)). The parameters used in the comparison are velocity v in the fracture of 1000 m/year, a matrix porosity ϕ of 2% in the rock matrix, a fracture aperture half width δ of 10^{-4} m, a reaction rate constant in the rock matrix k_m of 10^{-6} s^{-1} and a rate constant k_f of 0 in the fracture, and a diffusion coefficient in porous media D' of 10^{-6} cm^2 s^{-1}. A concentration profile versus distance for SiO_2(aq) is shown at 0.01 and 1.0 years for both the analytical solution (Eq. (29)) and for the numerical model (Fig. 2). The match between the analytical and numerical solution at 0.01 years is close but not perfect due to the numerical dispersion resulting from the upwind formulation for advective transport. At 1.0 years, however, the match is very good since the system has evolved close to the stationary-state solution where the effects of numerical dispersion in a one-dimensional system are negligible.

6. Stationary state solution

The stationary-state solutions for the fracture and the rock matrix (Eq. (30) Eq. (36)), respectively, can be obtained by letting $t \to \infty$ (and remembering that erfc(−∞) = 2 and erfc(∞) = 0). The solutions to the stationary state forms of Eq. (24) Eq. (23) can be expressed as

$$C_\mathrm{f}(z) = C_0 \mathrm{e}^{-z/\lambda_\mathrm{f}}, \tag{41}$$

and

$$C_\mathrm{m}(x,\ z) = C_\mathrm{f}(z)\mathrm{e}^{-x/\lambda_\mathrm{m}} = C_0 \mathrm{e}^{-z/\lambda_\mathrm{f}} \mathrm{e}^{-x/\lambda_\mathrm{m}}. \tag{42}$$

Taking the logarithm of both sides of Eq. (39), it is apparent that equal contours of the concentration are represented by

$$\frac{x}{\lambda_\mathrm{m}} + \frac{z}{\lambda_\mathrm{f}} = \mathrm{constant}. \tag{43}$$

Since the reaction is assumed to be linear ($r = kC$), Eq. (40) also gives an expression for constant contours of the reaction rate. For a quasi-stationary state system, the lines of constant concentration and reaction rate also mark the position of mineral fronts. This form of the analytical solution for the rock matrix, therefore, can be used to obtain an expression for the geometry of the mineral fronts in the rock matrix. The slope of the quasi-stationary state mineral fronts is equal to

$$\frac{\mathrm{d}x}{\mathrm{d}z} = -\frac{\lambda_\mathrm{m}}{\lambda_\mathrm{f}} = -\left(\frac{k_\mathrm{f}}{v}\lambda_\mathrm{m} + \frac{\phi D'}{v\delta}\right). \tag{44}$$

Or we can rewrite this expression in terms of the fracture equilibration length scale in the absence of matrix diffusion to yield

$$\frac{\mathrm{d}x}{\mathrm{d}z} = -\left(\frac{\lambda_\mathrm{m}}{\lambda_\mathrm{f}^0} + \frac{\phi D'}{v\delta}\right). \tag{45}$$

Note that the second term in brackets is independent of the kinetic rate constants and depends only on the fracture aperture, matrix porosity and diffusion coefficient, and the fracture fluid velocity. The first term is equal to the ratio of equilibration lengths for the matrix and the fracture in the absence of coupling to the matrix. This term written out becomes

$$\frac{\lambda_\mathrm{m}}{\lambda_\mathrm{f}^0} = \frac{k_\mathrm{f}}{v}\sqrt{\frac{\phi D'}{k_\mathrm{m}}}. \tag{46}$$

If we break up the effective rate constants k_m and k_f into an intrinsic rate constant (per unit surface area mineral), which is assumed the same in the matrix and the fracture, multiplied by a mineral surface area term given by A_m in the matrix and $1/\delta$ in the fracture, the effective rate constants become

$$k_\mathrm{f} = \frac{k}{\delta}, \tag{47}$$

and

$$k_\mathrm{m} = A_\mathrm{m} k. \tag{48}$$

Making use of these expressions along with Eq. (43), Eq. (42) becomes

$$\frac{\mathrm{d}x}{\mathrm{d}z} = -\left(1 + \sqrt{\frac{k}{A_\mathrm{m}\phi D'}}\right)\frac{1}{\mathrm{Pe.}} \tag{49}$$

Note that k has the units of m/s if D' is in units of m^2/s and A_m is in units of m^{-1}. With $D' = 10^{-9}$ m^2/s, $A_\mathrm{m} =$ 100 m^{-1}, and a porosity of 10%, the quantity under the square root is of order unity if

$$k \sim A_\mathrm{m}\phi D' \simeq 10^{-8}\,\mathrm{m s^{-1}}. \tag{50}$$

Note that with increasing flow velocity (Pe $\to \infty$) the slope of mineral fronts in the rock matrix decrease to zero (i.e., they become parallel to the fracture). For fixed Pe, as k increases the slope becomes infinite, or perpendicular to the fracture. Thus, it is interesting to note that for relatively small values of the rate constant k relative to the diffusion coefficient in the rock matrix (i.e., for surface reaction-controlled conditions), the slope of the mineral fronts in the rock matrix become independent of the rate constant

Table 1
Solute concentrations for the cement pore water used as a boundary condition in dual porosity calculation

Component	Concentration(mol/l)
Total Na	5.0×10^{-2}
Total Ca	1.7×10^{-2}
Total Mg	2.5×10^{-8}
Total CO_2	1.6×10^{-6}
Total Cl	5.0×10^{-3}
I(M)	9.7×10^{-2}
Alkalinity	3.49×10^{-2}
T (°C)	25
pH	12.39
log P_{CO_2}	− 12.90

whereas for large rate constants approaching local equilibrium the slope is dependent on the rate constant. Although these results apply rigorously to a one-component stationary state system in which the reaction can be described with a linear rate law, the relationships derived here may be useful for more general multicomponent systems as we shall show below.

7. Alteration front geometries in multicomponent systems

The analytical solution for the stationary state discrete fracture system given above (Eq. (39)) was used to obtain an expression for the slope of the reaction fronts (Eq. (46)). The analytical solution, however, is strictly applicable to a system characterized by a single chemical component and by linear kinetics. Here we use the numerical code described above to see whether the same expression can be used to calculate alteration front geometry in a more complicated (nonlinear) case involving precipitation and dissolution. As an example, we consider an idealized case in which hyperalkaline groundwaters infiltrate a calcitic dolomite along fractures. The situation is similar to that considered by Steefel and Lichtner (1994), except that we neglect silicate phases in order to keep the analysis simple. As a boundary condition at the origin of the fracture, we use a groundwater equilibrated with portlandite, brucite, and calcite, giving a pH of 12.39 (Table 1). As an initial condition in the rock matrix and fracture (to which the system is not particularly sensitive), we use a typical Na–HCO_3 groundwater composition in equilibrium with the calcite and dolomite in the rock (Table 2). In addition, we

Table 2
Solute concentrations used as an initial condition in the calculations

Component	Concentration(mol/l)
Total Na	5.0×10^{-2}
Total Ca	9.7×10^{-4}
Total Mg	6.1×10^{-5}
Total CO_2	2.0×10^{-3}
Total Cl	5.0×10^{-2}
I(M)	5.3×10^{-2}
Alkalinity	2.0×10^{-3}
T (°C)	25
pH	8.00
log P_{CO_2}	− 3.0

Table 3
Reaction rate constants and surface areas used in the calculations

Mineral	Log k_s (moles/m^2/s)	Surface area (m^2/m^3)	Reference
Calcite	− 6.19	500	Chou et al. (1989)
Dolomite	− 7.70	500	Busenberg and Plummer (1982)
Brucite	− 8.00	500	

Table 4
Reactions and equilibrium constants used in the calculations

Reaction	log K_{eq}
$OH^- + H^+ \rightleftharpoons H_2O$	14.00
$HCO_3^- \rightleftharpoons CO_3^{-2} + H^+$	− 10.33
CO_2 (aq) $\rightleftharpoons CO_3^{-2} + 2H^+$	− 16.67
$NaHCO_3$ (aq) $\rightleftharpoons CO_3^{-2} + H^+ + Na^+$	− 10.48
$NaCO_3^- \rightleftharpoons CO_3^{-2} + Na^+$	− 0.51
NaOH (aq) + $H^+ \rightleftharpoons Na^+ + H_2O$	14.80
$MgCO_3$ (aq) $\rightleftharpoons CO_3^{-2} + Mg^{+2}$	− 2.98
$MgHCO_3^+ \rightleftharpoons CO_3^{-2} + Mg^{+2} + H^+$	− 11.37
$MgOH^+ + H^+ \rightleftharpoons Mg^{+2} + H_2O$	11.79
MgCl + $\rightleftharpoons Mg^{+2} + Cl^-$	0.13
$CaHCO_3^+ \rightleftharpoons CO_3^{-2} + Ca^{+2} + H^+$	− 11.38
$CaOH^+ + H^+ \rightleftharpoons Ca^{+2} + H_2O$	12.85
Calcite $\rightleftharpoons Ca^{+2} + CO_3^{-2}$	− 8.48
Dolomite $\rightleftharpoons Ca^{+2} + Mg^{+2} + CO_3^{-2}$	− 18.14
Brucite + $2H^+ \rightleftharpoons Mg^{+2} + 2H_2O$	16.30
Portlandite + $2H^+ \rightleftharpoons Ca^{+2} + 2H_2O$	22.56

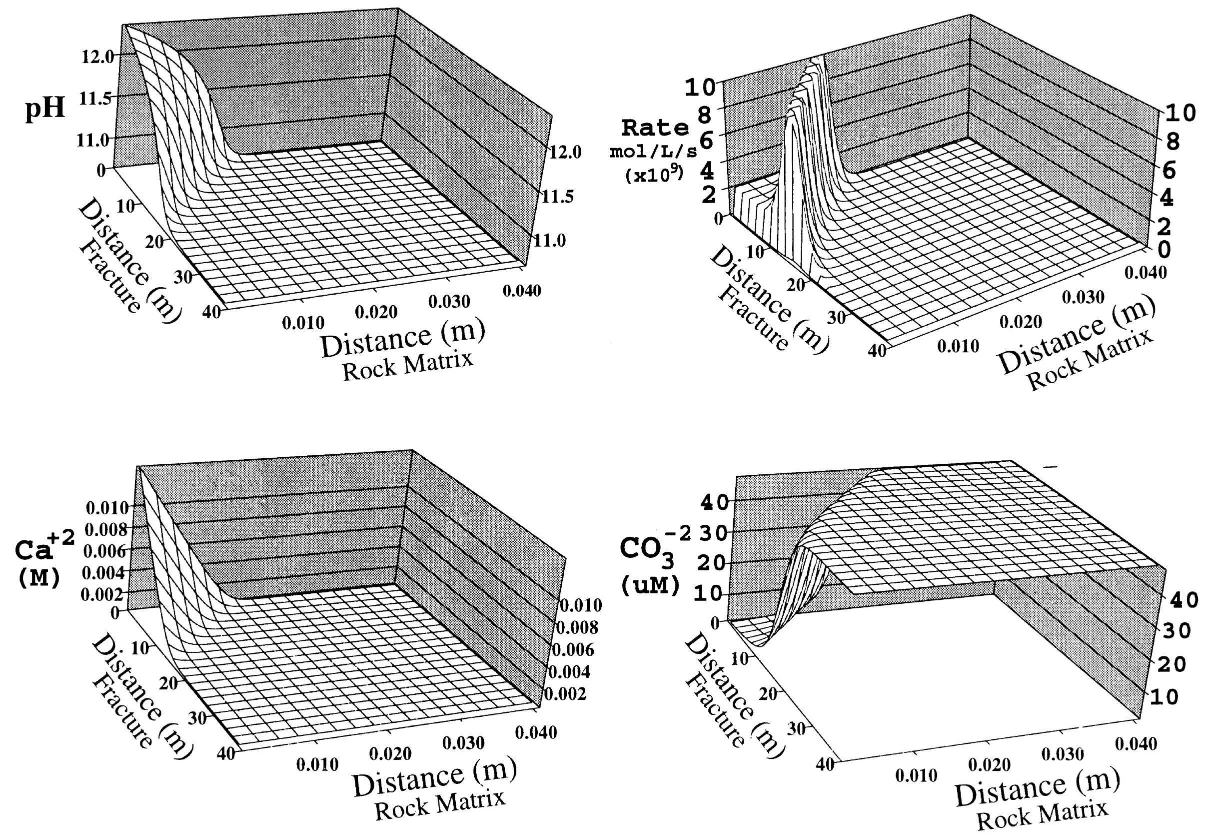

Fig. 3. Solution pH, calcite precipitation rate (mol/l/s × 10^9), CO_3^{-2} ion, and Ca^{+2} ion concentrations for 2D discrete fracture system. Note the wedge-shaped geometry in which both reaction fronts and solute isoconcentration lines intersect the fracture downstream of the fracture inlet.

assume that calcite, dolomite, and porosity make up 20, 50, and 30% of the rock, respectively. Mineral rate constants and surface areas used in the calculation are given in Table 3. Equilibrium constants for mineral and aqueous complexation reactions are given in Table 4. An effective diffusion coefficient of 10^{-10} m^2/s, a fracture aperture half-width of 0.946 mm, and a velocity in the fracture of 1000 m/year are assumed. This gives a value of 1000 for the quantity Pe defined by $\delta v/\phi D'$. A constant grid spacing of 1 m along the fracture and 0.5 mm perpendicular to the fracture are used to discretize the domain. Mineral dissolution and precipitation reactions are not allowed to affect the transport properties of the rock in this calculation. In Fig. 3, contour plots of the calcite precipitation rate, Ca^{+2}, CO_3^{-2}, and solution pH are shown at 50 years in the full discrete fracture (2D) system. Note the characteristic wedge-shaped geometry of the fronts which intersect the fracture downstream of the fracture inlet. Alteration envelopes are widest in the rock matrix close to the fracture inlet and become narrower with distance down the fracture. The distance at which a particular alteration front or solute isoconcentration line intersects the fracture is controlled by the parameter $\delta v/\phi D'$ (= 1000). This can be seen even more clearly by comparing pH profiles and calcite precipitation rates in the fracture with the pH and calcite rates from the rock matrix at $z = 0$ with distances scaled by 1000. (Fig. 4). The slight discrepancy that does exist is due to the coarser grid and resulting numerical dispersion in the fracture. Note that the calcite precipitation rate shows a peak at about 20 m down the fracture which corresponds to 2 cm in the rock matrix. This same behavior was observed in the more extensive calculations presented in

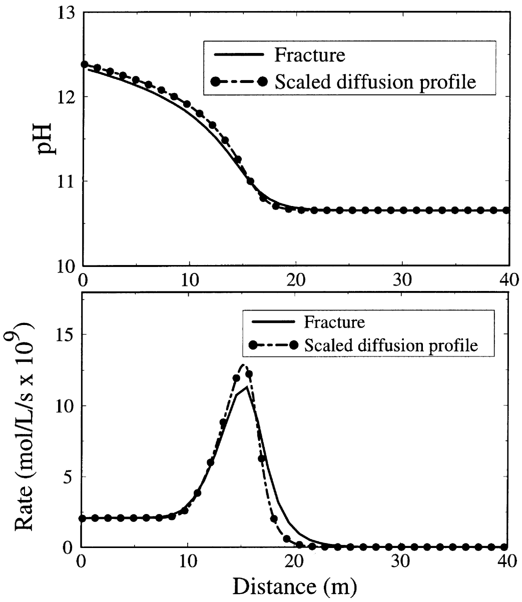

Fig. 4. Comparison of solution pH and calcite precipitation rate in the fracture with these respective quantities in the rock matrix, scaled by the parameter $\delta v/\phi D'$ (= 1000 in this example).

Steefel and Lichtner (1994) and is attributed to interdiffusion of Ca^{+2} and CO_3^{-2} ions resulting from the changing stoichiometry of the dedolomitization reaction as a function of distance from the fracture wall. Steefel and Lichtner (1994) showed that the distinctive topology of the calcite precipitation peak only occurs in a diffusion-dominated system. The peak is completely absent in an advection-dominant system. The discrete fracture results shown here indicate that even though advection is the dominant mode of transport in *the fracture itself*, the coupling to diffusion and reaction in the rock matrix results in a diffusion-controlled topology in the fracture. The results also indicate that, at least in theory, solute concentration, reaction rate, and volume fraction profiles along the fracture can be predicted from the one-dimensional reaction-diffusion calculation in the rock matrix by using the scaling factor Pe($\delta v/\phi D'$).

8. Discussion

The calculations described above suggest that the geochemical behavior of reactive species in fractured rock may differ substantially from that expected in homogeneous porous media. The principal conclusion from the modeling is that concentration profiles for major and minor species in fractures may be strongly affected by matrix diffusion and reaction, no matter what the length scale of the fracture itself. Using the example of infiltration of a hyperalkaline plume into a calcitic dolomite, we have shown that the concentration and mineral reaction rate profiles in the fracture show the same topology as do the concentration and mineral reaction rate profiles in the rock matrix where transport is purely via diffusion. In contrast, reactive transport in homogeneous porous media at these length scales results in advection as the dominant process, giving a substantially different profile (Steefel and Lichtner, 1994). The conclusion, therefore, is that the profiles in the fracture under quasi-stationary-state conditions may be 'diffusion- controlled', whatever the length of the fracture itself.

The aspect ratio of a reaction front in the rock matrix under surface reaction-controlled conditions is determined by the parameter $\phi D'/\delta v$. The analytical theory for a single component system with linear kinetics predicts in addition that the reaction fronts in the rock matrix will be straight lines. Similar behavior is seen in the geochemical system we have investigated here, despite the fact that the rate laws are nonlinear and the chemical system is multicomponent. Based on these results, the discrete fracture calculations suggest that it is possible to describe the quasi-stationary state system with a single one-dimensional reaction-diffusion calculation (even if multicomponent) in the rock matrix and a knowledge of the parameter $\phi D'/\delta v$. At the very least, this gives what appears to be a reliable way of making estimates of how a single fracture system will behave, since it will be possible to extract such important features of the system as the equilibration length scale and the distance required for groundwater pH values to reach near neutral values.

9. Conclusions

Using a combination of analytical solutions and numerical modeling of multicomponent reactive transport in a discrete fracture system, we have shown that the topology of reaction rate and concentration profiles in fractures may be diffusion-controlled, despite the high rates of solute transport in the fractures. Reaction front geometry in discrete fracture systems can be described in surface reaction-controlled systems with the parameter $\phi D'/\delta v$. This parameter, which does not depend on mineral reaction kinetics, is in fact a scaling factor which can be used to predict the distribution of concentrations and mineral zones in the fracture with a knowledge of the diffusion-controlled mineral zoning in the rock matrix. Practical use of this result might be to predict mineralization along a fracture from field observations of wall rock alteration.

Acknowledgements

The authors are grateful to Nick Waber and Carol Bruton for their careful reviews of the manuscript. We are pleased to acknowledge the support of the Schweizerischer Nationalfonds in the form of a grant (21-30908.91) to Peter C. Lichtner which funded a one-year post-doctoral position for the senior author at the Universität Bern in Switzerland. We are also grateful for the additional financial support provided by Professor Tjerk Peters of the Mineralogisch-Petrographisches Institut at the Universität Bern and by Drs Ian McKinley and Russel Alexander at the Nationale Genossenschaft für die Lagerung radioaktiver Abfälle (NAGRA).

References

Aagaard, P., Helgeson, H.C., 1982. Thermodynamic and kinetic constraints on reaction rates among minerals and aqueous solutions. I: Theoretical considerations, Amer. J. Sci., 282, 237–285.

Bear, J., 1979. Hydraulics of Groundwater. McGraw-Hill, New York, p. 569.

Busenberg, E., Plummer, L.N., 1982. The kinetics of dissolution of dolomite in CO_2–H_2O systems at 1.5 to 65°C and 0 to 1 ATM P_{CO_2}, Amer. J. Sci., 282, 45–78.

Cacas, M.C., Ledoux, E., de Marsily, G., Barbreau, A., Calmels, P., Gaillard, B., Margritta, R., 1991. Modelling fracture flow with a stochastic discrete fracture network: calibration and validation, 2: The transport model, Water Resources Res., 26, 491–500.

Chou, L., Garrels, R.M., Wollast, R., 1989. Comparative study of the kinetics and mechanisms of dissolution of carbonate minerals, Chemical Geology, 78, 269.

Cvetkovic, V.D., 1991. Mass arrival of reactive solute in single fractures, Water Resources Res., 27, 177–183.

de Marsily, G., 1986. Quantitative Hydrogeology. Academic Press, New York, p. 440.

Dove, P.M., 1995, Kinetic and thermodynamic control on silica reactivity in weathering environments. In Chemical Weathering Rates of Silicate Minerals, Reviews in Mineralogy (eds. A.F. White and S.L. Brantley), Mineral. Soc. Am. 31, 235–290.

Dullien, F.A.L., 1979. Porous Media. Academic Press, San Diego, p. 396.

Dykhuizen, R.C., 1992. Diffusive matrix fracture coupling including the effects of flow channeling, Water Resources Res., 28, 2447–2450.

Ge, S., 1997. A governing equation for fluid flow in rough fractures, Water Resources Res., 33, 53–61.

Kirkner, D.J., Reeves, H., 1988. Multicomponent mass transport with homogeneous and heterogeneous chemical reactions: effect of chemistry on the choice of numerical algorithm I. Theory, Water Resources Res., 24, 1719–1729.

Lasaga, A.C., 1981. Rate laws in chemical reactions. In: Lasaga, A.C., Kirkpatrick, R.J. (Eds.), Kinetics of Geochemical Processes. Rev. Mineral 8, 135–169.

Lasaga, A.C., 1984. Chemical kinetics of water–rock interactions, J. Geophys. Res., 89, 4009–4025.

Lichtner, P.C., 1985. Continuum model for simultaneous chemical reactions and mass transport in hydrothermal systems, Geochim. Cosmochim. Acta, 49, 779–800.

Lichtner, P.C., 1988. The quasi-stationary state approximation to coupled mass transport and fluid–rock interaction in a porous medium, Geochim. Cosmochim. Acta, 52, 143–165.

Lichtner, P.C., 1991. The quasi-stationary state approximation to fluid/rock reaction: local equilibrium revisited. In Ganguly, J. (Ed.), Diffusion, Atomic Ordering, and Mass Transport. Advances in Physical Geochemistry 8, 454–562.

Maloszewski, P., Zuber, A., 1993. Tracer experiments in fractured rocks: matrix diffusion and the validity of models, Water Resources Res., 29, 2723–2735.

McKinley, I., Alexander, W.R., 1993. Assessment of radionuclide retardation: uses and abuses of natural analogue studies, J. Contam. Hydrol., 14, 249–261.

Moreno, L., Neretnieks, I., 1993. Fluid flow and solute transport in a network of channels, J. Contam. Hydrol., 14, 163–192.

Moreno, L., Neretnieks, I., Eriksen, T., 1985. Analysis of some laboratory tracer runs in natural fissures, Water Resources Res., 21, 951–958.

Moreno, L., Tsang, Y.W., Tsang, C.F., Hale, F.V., Neretnieks, I., 1988. Flow and tracer transport in a single fracture—a stochastic model and its relation to some field observations, Water Resources Res., 24, 2033–2048.

Moreno, L., Tsang, C.F., Tsang, Y.W., Neretnieks, I., 1990. Some anomalous features of flow and solute transport arising from fracture aperture variations, Water Resources Res., 26, 2377–2391.

Nagy, K.L., 1995, Dissolution and precipitation kinetics of sheet silicates. In: Chemical Weathering Rates of Silicate Minerals, Eds. A.F. White and S.L. Brantley, Rev. Mineral. 31, 173–233.

Neretnieks, I., 1980. Diffusion in the rock matrix: an important factor in radionuclide retardation?, J. Geophys. Res., 85, 4379–4397.

Neretnieks, I., Eriksen, T., Tahtinen, P., 1982. Tracer movement in a single fissure in granitic rock: some experimental results and their interpretation, Water Resources Res., 21, 849–858.

Nordqvist, A.W., Tsang, Y.W., Tsang, C.F., Dverstorp, B., Andersson, J., 1996. Effects of high variance of fracture transmissivity on transport and sorption at different scales in a discrete model for fractured rocks, J. Contam. Hydrol., 22, 39–66.

Norton, D., Knapp, R., 1977. Transport phenomena in hydrothermal systems: the nature of porosity, Amer. J. Sci., 277, 913–936.

Novak, C.F., 1996. Development of the FMT chemical transport simulator: coupling aqueous density and mineral volume fraction to phase compositions, J. Contam. Hydrol., 21, 297–310.

Novak, C.F., Sevougian, S.D., 1992, Propagation of dissolution/precipitation waves in porous media. In: Migration and Fate of Pollutants in Soils and Subsoils (D. Petruzzelli, F.G. Helfferich, eds.) NATO ASI Series. Series G: Ecological Sciences, 32, Springer-Verlag, Berlin: 275–307.

Odling, N.E., Roden, J.E., 1997. Contaminant transport in fractured rocks with significant matrix permeability, using natural fracture geometries, J. Contam. Hydrol., 27, 263–283.

Park, C.K., Vandergraaf, T.T., Drew, D.J., Hahn, P.S., 1997. Analysis of the migration of nonsorbing tracers in a natural fracture ingranite using a variable aperture channel model, J. Contam. Hydrol., 26, 97–108.

Phillips, O.M., 1991, Flow and reactions in permeable rocks. Cambridge University Press, Cambridge, UK, 285 p.

Reed, M.H., 1982. Calculation of multicomponent chemical equilibria and reaction processes in systems involving minerals, gases, and an aqueous phase, Geochim. Cosmochim. Acta, 46, 513–528.

Skagius, K., Neretnieks, I., 1986. Porosities and diffusivities of some nonsorbing species incrystalline rocks, Water Resources Res., 22, 389–398.

Smellie, J.A.T., Karlsson, F., Alexander, W.R., 1997. Natural analogue studies: present status and performance assessment implications, J. Contam. Hydrol., 26, 3–18.

Snow, D.T., 1968. Rock fracture spacings, openings, and porosities. J. Soil Mech., Found Div., Proc. Amer. Soc. Civil Engrs., v. 94, 73–91.

Steefel, C.I., Lasaga, A.C., 1994. A coupled model for transport of multiple chemical species and kinetic precipitation/dissolution reactions with application to reactive flow in single phase hydrothermal systems, Amer. J. Sci., 294, 529–592.

Steefel, C.I., Lichtner, P.C., 1994. Diffusion and reaction in a rock matrix bordering a hyperalkaline fluid-filled fracture, Geochim. Cosmochim. Acta, 58, 3595–3612.

Steefel, C.I., Lichtner, P.C., 1998. Multicomponent reactive transport in discrete fractures: II. Infiltration of hyperalkaline groundwater at Maqarin, Jordan, a natural analogue site. J. Hydrology, 209, 200–224.

Steefel, C.I., MacQuarrie, K.T., 1996. Approaches to modeling reactive transport in porous media. In: Lichtner, P.C., Steefel, C.T., Oelkers, E.H. (Eds.), Reactive Transport in Porous Media, Reviews in Mineralology 34. Mineral. Soc. Am. 83, 83–129.

Steefel, C.I., Van Cappellen, P., 1990. A new kinetic approach to modeling water–rock interaction: the role of nucleation, precursors, and Ostwald ripening, Geochim. Cosmochim. Acta, 54, 2657–2677.

Steefel, C.I., Yabusaki, S.B., 1996. OS3D/GIMRT, Software for Multicomponent–Multidimensional Reactive Transport, User Manual and Programmer's Guide, PNL-11166. Pacific Northwest National Laboratory, Richland, Washington.

Tang, D.H., Frind, E.O., Sudicky, E.A., 1981, Contaminant transport in fractured porous media: analytical solution for a single fracture. Water Resources Res. 17, 555–564.

Therrien, R., Sudicky, E.A., 1996. Three-dimensional analysis of variably-saturated flow and solute transport in discretely-fractured porous media, J. Contam. Hydrol., 23, 1–44.

Thoma, S.G., Gallegos, D.P., Smith, D.M., 1992. Impact of fracture coatings on fracture/matrix flow interactions in unsaturated, porous media, Water Resources Res., 28, 1357–1367.

Tsang, Y.W., Tsang, C.F., 1989. Flow channeling in a single fracture as a two-dimensional strongly heterogeneous permeable medium, Water Resources Res., 25, 1076–2080.

Vandergraaf, T.T., Drew, D.J., Archambault, D., Ticknor, K.V., 1997. Transport of radionuclides in natural fractures: some aspects of laboratory migration experiments, J. Contam. Hydrol., 26, 83–95.

Yeh, G.T., Tripathi, V.S., 1989. A critical evaluation of recent developments in hydrogeochemical transport models of reactive multichemical components, Water Resources Res., 25, 93–108.

Yeh, G.T., Tripathi, V.S., 1991. A model for simulating transport of reactive multispecies components: model development and demonstration, Water Resources Res., 27, 3075–3094.